Journal of Thermal Analysis and Calorimetry, Vol. 85 (2006) 3, 531–540

NEW DEVELOPMENTS AND APPLICATIONS IN TITRATION CALORIMETRY AND REACTION CALORIMETRY

F. Dan[1], *M. H. Hamedi*[2] *and J-P. E. Grolier*[3*]

[1]Department of Macromolecular Chemistry, Gh.Asachi Technical University, 71 Mangeron Ave., 700050 Iasi, Romania
[2]Mechanical Engineering Department, K.N. Toosi University of Technology, East Vafadar Ave. Tehran, Iran
[3]Laboratory of Thermodynamics of Solutions and Polymers, University Blaise Pascal, 24 des Landais Ave., 63177 Aubière, France

Isothermal titration calorimetry (ITC) and reaction calorimetry (RC) have been used to construct the solid-liquid equilibrium line in ternary systems containing the solute to precipitate and an aqueous mixed solvent, and to study polymerization reactions under real process conditions, respectively. Phase diagrams have been established over the whole concentration range for some benzene substituted derivatives, including *o*-anisaldehyde, 1,3,5-trimethoxybenzene and vanillin, in {water + alcohol}mixtures at different temperatures. Acrylamide polymerization in aqueous solution using potassium permanganate/acid oxalic redox system as initiator was investigated on a homemade calorimeter, which works according to the isoperibolic mode. A Calvet type differential RC was used to illustrate the applicability of temperature oscillation calorimetry (TOC) for the evaluation of the heat transfer coefficient during the course of reaction.

Keywords: *acrylamide polymerization, calorimeter time constant, heat of dissolution/reaction, heat transfer coefficient, solid-liquid equilibrium, solubility, ternary systems, titration/reaction calorimetry, viscosity changes*

Introduction

Calorimetric methods have been an invaluable tool for understanding many physical and chemical phenomena either in the early phases of process development or in biological applications. Alongside of differential scanning calorimetry (DSC), isothermal titration and reaction calorimentry are the widely used calorimetric techniques.

Titration calorimetry has been traditionally used for titration or acid-base reactions [1]. ITC is also currently used to study complex formation in pharmaceutical applications and binding effects in biophysical applications. Numerous examples of such investigations using ITC can be found in recent publications where different calorimeters have been used [2–5]. Recently, the advent in several highly sensitive titration calorimeters has generated much interest in this technique [6–9]. Titration calorimetry has been very rarely used to measure solubilisation or dissolution of solid compounds. However, Smith and coworkers [10–12] have used ITC to establish solubility boundaries in complex systems like microemulsions. The present study takes place in the general approach regarding the design and the development of methods useful for the acquisition of thermodynamic data on phase equilibria in crystallization engineering. Crystallization is of particular interest since it constitutes very often the final step of the solids purification. A rigorous control of temperature is essential in solubility phenomena then isothermal experimental techniques should be favoured. The construction of a phase diagram containing a solid solute and a liquid solvent is simply based on the determination of the solubility of the solid solute in the solvent. The solvent can be a pure liquid component or a liquid mixture for efficient solvent-antisolvent selective capability. The choice of selected solvents in crystallization processes rests on the knowledge of the solid phase contour of the product to precipitate in the presence of the solvent-antisolvent mixture. Since theoretical calculations are not available so far to provide accurate prediction of the solubility limits of a solid component in binary mixtures, experimental determinations are necessary to establish solid-liquid phase equilibria in ternary systems. When the solute is an organic component the solvent is generally a binary mixture water + a hydrophilic organic component. The thermodynamic study of the whole system is focused on the determination of the maximum of solubility of the solid solute that is to say all along the solid-liquid line of the ternary system; in this way, this line which is the locus of the maximum solubility data points is readily obtained as of plot of those points. In this context, the solubility limit was determined by adding slowly (to remain at thermodynamic

* Author for correspondence: j-pierre.grolier@univ-bpclermont.fr

1388–6150/$20.00

Akadémiai Kiadó, Budapest, Hungary
Springer, Dordrecht, The Netherlands

equilibrium) successive small increments of the binary solvent to a known (weighted) amount of the solid solute until the complete dissolution of the solid crystals. One of the important aspects of this work was the use of titration calorimetry to detect the dissolution of the solid in the binary solvent through the heat involved during each addition. Phase diagrams have been established over the whole concentration range for some benzene substituted derivatives, including *o*-anisaldehyde, 1,3,5-trimethoxybenzene and vanillin, in water + methanol, + ethanol, or + propanol. The effect of temperature was examined through measurements in the temperature range 303 to 318 K.

On its side, RC is the technique accepted as the most powerful way to study the chemical processes in near-to-the-industrial conditions, allowing a wide spectrum of operation conditions and measurements. The second objective of this work was to validate a small scale isoperibolic calorimeter aim of be used for studying polymerizations. In the isoperibolic mode the surroundings of the reaction mass (usually a jacket) are maintained at constant temperature. Exothermic or endothermic changes will produce a temperature increase or decrease in the reactor. The basic equation of RC is the heat balance of a reactor with external cooling jacket, under the hypothesis of perfect mixing in the reactor and in the jacket it, is the following:

$$C_p \frac{dT_r}{dt} = UA(T_j - T_r) + Q_{chem} + Q_{loss} + Q_{dos} + P_{stirrer} \quad (1)$$

In the simplest case, the heat transfer coefficient, *UA*, is assumed as constant and it is obtained by carrying out an initial calibration experiment with a calibration heater. When the heat loss, Q_{loss}, and the power dissipated by the stirrer, $P_{stirrer}$, are known or negligible, Eq. (1) allows the evaluation of the heat of reaction [13]. Instead, when the heat transfer coefficient undergoes large changes, for example in batch reactors, as a consequence of increase of viscosity, the heat of reaction, Q_{chem}, cannot be computed from Eq. (1), unless the variation of heat transfer coefficient is known. The increase in viscosity during polymerization is almost negligible in suspension and moderate in heterogeneous bulk polymerizations but significant changes occur in homogeneous bulk or solution polymerization [14]. This is why the homogeneous solution polymerization of acrylamide (AM) was chosen as model to illustrate the performances and the limits of the new RC. In the present work our attention was focused on the interpretation of the measured signals in order to achieve reliable calorimetric data. Thus, the evolution of the heat transfer coefficient was followed by performing two calibration experiments, before and after the reaction; the two values of the heat transfer coefficient were subsequently interpolated, by to obtain the desired $UA(t)$ profile. Using the heat pulse calibration, a differentiation method based on the convolution of the measured heat flow by the generated one was used for determining the time constants and deconvoluting the measured heat flow.

The last objective of this work was to develop the Temperature Oscillation Calorimetry (TOC) technique particularly in a small volume (9 mL) reactor using a Calvet-type differential calorimeter. The aim of this calorimetric technique was to obtain on-line the parameters involved in the heat balance of the reaction mass during a chemical reaction.

Experimental

Chemicals

4-Hydroxy-3-methoxybenzaldehyde (or vanillin) with 99 mol% purity, *o*-anisaldehyde with 98 mol% purity and 1,3,5-trimethoxybenzene with 99 mol% purity respectively were provided by (Fine Chemicals) Acros Organics France; methyl alcohol with purity >99.8 mol% was provided by Fluka Chemika France; ethyl alcohol absolute RE was provided by Carlo Erba France; propyl alcohol p.a. with purity >99.5 mole% was provided by (Fine Chemicals) Acros Organics France. All chemicals were used without further purification. Solutions were prepared by mass using freshly bidistilled water. Acrylamide (AM), potassium permanganate and oxalic acid, used for polymerizations, were provided by Fluka Chemika, France and were used without further purification.

Instrumentation

The titration calorimeter, Titrys model, commercialized by Setaram was used to perform the solubility measurements. The calorimeter is built according to the Calvet principle. The calorimetric block whose temperature can be regulated to ±20 mK houses two thermopiles in which are placed the measuring and reference cells respectively. The differential detection allows to detect heat effects with 0.1 μW sensitivity. The instrument can be operated in the temperature range from 303.15 to 330.15 K. For this application the calorimeter (see a schematic view of the calorimeter in Fig. 1a) presents a double interesting feature: in each cell an active volume from 1 up to 12 cm^3 can be used and the content of each cell can be stirred by means of a small magnetic bar activated by a single small motor which ensures the same (adjustable) stirring speed in both cells. The calorimeter can be fed with an injection system Dual Syringe Pump Model

33 from Harvard, composed of two identical syringe pumps mounted on a dual carriage in such a way that identical volumes delivered by stainless capillaries can be injected simultaneously at exactly the same rate in both cells; during each injection the corresponding heat effect is recorded as shown in Fig. 2a. The injection system is entirely programmable and computer controlled. In order to ensure a better control of the volumes delivered by the pumps, the whole assembly, syringe pumps and their carriage/holder, were placed in a small air bath thermostated to ±50 mK. Before injection in the calorimetric cells, liquids coming from the pumps are further thermostated as the feeding capillaries are coiled in two small thermostats placed inside the calorimetric block on top of each cell (see details in Fig. 1a).

The set-up of the designed reaction calorimeter is depicted in Fig. 1b. The reactor is a 100 mL flask with a jacket and a lid with five ports. The flask jacket is connected to a thermostatic bath whose temperature is maintained within ±0.1°C with a Vertex (model V9610) PID controller. One temperature sensor (Pt100) is placed in the reactor and two more at the jacket inlet and outlet, respectively. An additional J-type thermocouple (1 mm external diameter) is placed in the space between the lid and the liquid's surface. As the details of Fig. 1b shows, the thermocouple is in intimate contact with the feeding tube and consequently with liquid containing the initiator solution. Since, usually, the temperature of dosed liquid is below the reaction temperature, the decrease of temperature to the thermocouple serves as trigger for the start of reaction as well as to correct the Q_{chem} by the heat exchanged with the reaction mass during reagents dosing, Q_{dos} in Eq. (1). The reactor also holds the calibration heater (electric resistance of 15 Ω) powered by a 30V/1A power supplier via a power amplifier connected to one of the analog outputs of the data acquisition board (a PCI-441D model from Datel Inc., USA). We developed a LabVIEW® (National Instruments) to generate a desired voltage which is applied to the resistor during the calibration periods. For the sake of brevity, the desired amount of heat (in Joules) and the suited voltage are introduced by the operator via the front panel of LabVIEW software. The power uptake of the heater is measured on-line, integrated over the time and compared with the required amount of heat. As soon as the two values are equal each to other a digitally controlled relay stops the current passing through the heater. In semibatch operation mode the reagent is fed over a period with a peristaltic pump (MasterFlex C/L, Barnant Company, USA) with a pre-calibrated feeding rate. The duration of feed is controlled by the software through a computer controlled relay. The whole application is controlled by a single LabVIEW program running on computer. The program allows direct interaction with all devices connected to the system as well as automatic handling of a pre-defined recipe. The main task of the LabVIEW program is to acquire the data of all sensors and devices as well as to control the stirrer speed and the power dissipated by the calibration

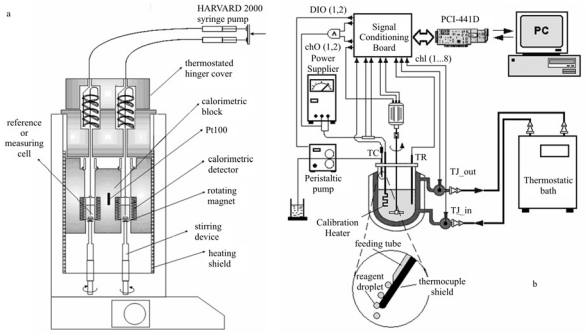

Fig. 1 General view of a – the Titrys titration calorimeter, showing the differential mounting of the thermopiles housing the calorimetric cells, the thermostated lid (in the upper position) and the injection dual syringe; and b – schematic illustration of the isoperibolic reaction calorimeter. In the lower part of scheme a detail of the assembly thermocouple-feeding tube used as trigger for the zero moment of polymerization is given

Table 1 Signal-conditioning specification of the measured input data with the isoperibolic RC

Signal	Channels	Description	Amplified	Filter
TR	chO_1	Reaction Temperature (Pt100 sensor)	yes	4Hz
*TJ*_in *TJ*_out	chO_2, 3	Jacket Temperatures at inlet and outlet (Pt100 sensors)	yes	4Hz
I_{ch}	chO_4	Current passing through the calibration heater	no	no
V_{ch}	chO_5	Voltage supplied through the calibration heater		
TC	chO_6	Dosing liquid temperature (J-type thermocouple)	yes	4Hz
I_{Stirr}	chO_7	Current required by the stirrer engine to maintain the desired stirring speed	yes	no
V_{Stirr}	chO_8	Voltage uptake by the stirrer engine	no	no

heater. Both tasks are performed by the same PCI-441D precision sensor input and multi-functional I/O board. The different signals acquired by the computer are given in Table 1. The two analog outputs are used to control the stirrer speed and the power dissipated by the calibration heater, respectively.

Experimental procedures

In ITC, an initial mass, usually 0.50 g of finely ground powder is placed in the measuring cell. The two syringe pumps are filled with the same water-alcohol solution of known composition. A dissolution run consists in adding the same volume of the solution simultaneously in both cells. The change in enthalpy evolved during each addition is due to the heat of dissolution of part of the solid in the small amount of added solution; this is directly given by the differential heat flow recorded upon injection of the solution. Typically, each injection consists in adding 0.20 cm^3 of solution at the rate of 0.10 cm^3 min^{-1} and a complete run is achieved after an average of 10 successive additions. Each run yields a series of heat peaks (as shown in Fig. 2a). The different heat effects ΔH, the actual peak areas, are plotted *vs*. the number $\alpha=n_{solvent}/n_{solute}$ which represents the ratio of the number of moles of solvent to the number of moles of the solute. Then, each dissolution run yields the type of plot shown in Fig. 2b. Typically each experiment is composed of two parts. First an increase of ΔH represented by a linear function with α: $\Delta H/n_1=A_1\alpha$. Then, when all the solid has been completely solubilized, the second part which is simply related to the heat of dilution of the medium, is generally well represented by a polynomial of the form: $\Delta H/n_1=A'_0+A'_1\alpha+A'_2\alpha^2$. The coefficients A_1, A'_0, A'_1, A'_2 were determined by linear regression. The intercept of the two parts gives the enthalpy of dissolution for a given ratio α_S at saturation, Eq. (2):

$$A_1\alpha_S = A'_0+A'_1\alpha_S+A'_2\alpha_S^2 \qquad (2)$$

From α_S at saturation, the composition of the ternary system at saturation can be determined as follows:

$$\alpha_S = n_{solvent}/n_1 = (n_2+n_3)/n_1 = (x_2+x_3)/x_1 \qquad (3)$$

where n_i is the number of moles of each component.

Since $x_1+x_2+x_3=1$ one can finally write: $a_S=(1-x_1)/x_1$ and $x_1=1/(\alpha_S+1)$, $x_2=x_{2,S}(1-x_1)$ and $x_3=x_{3,S}(1-x_1)$, respectively.

The dissolution runs are made in such a way as to cover the whole concentration of the binary aqueous mixture. Then a ternary plot (x_1, x_2, x_3) can be constructed where the three mole fractions are the actual experimental mole fractions corresponding to the individual coordinates of the different intercepts.

With RC, a typical polymerization experiment is presented in Fig. 3a. The reactor jacket was fixed at the working temperature, the monomer and the solvent are charged in the calorimetric vessel and as soon as the thermal equilibrium is reached the solutions of $KMnO_4/H_2C_2O_4$ redox system are fed using the dosing pump. As shown in Fig. 3a, the polymerization does not start in the presence of $KMnO_4$ (the first endothermic peak of the temperature recorded by thermocouple) but it starts soon after the dosing of oxalic acid. The maximum increase of temperature of the reaction mass ($\Delta T_R=T_R-T_{J\_}out$) was about 7.3°C. In order to quantify the heat of reaction, the correlation between the temperature difference and the corresponding heat flow should be made. A known amount of power P (up to 10 W) is dissipated through the resistance of the calibration heater during a well-defined

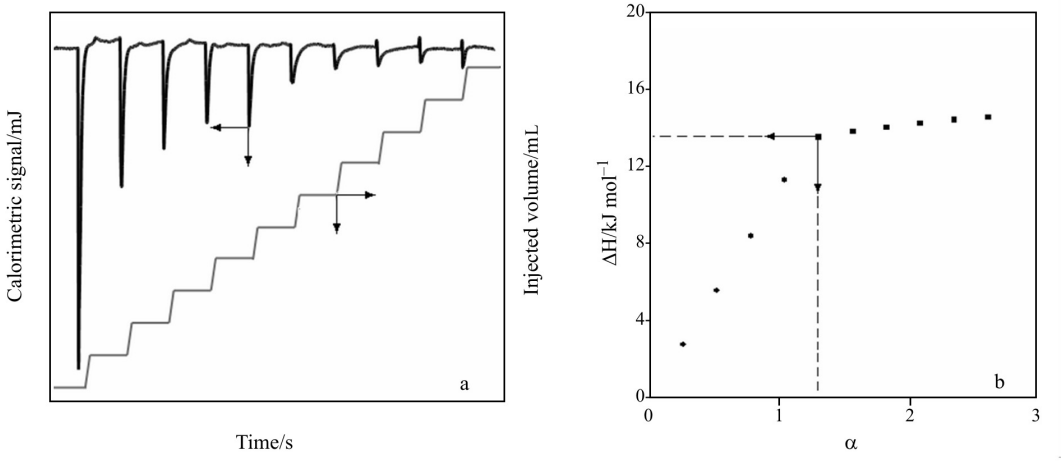

Fig. 2 Calorimetric signal *vs*. injected volume of solvent, showing thermal traces of heat effects a – obtained upon successive additions; and b – plot of cumulated thermal effects, ΔH/kJ mol^{-1} *vs*. $\alpha=n_{solvent}/n_{solute}$, obtained during a run, showing the initial dissolution ● – of the solid solute followed by the dilution ■ – of the solution. The intercept gives the enthalpy of dissolution and the ratio α_s at saturation

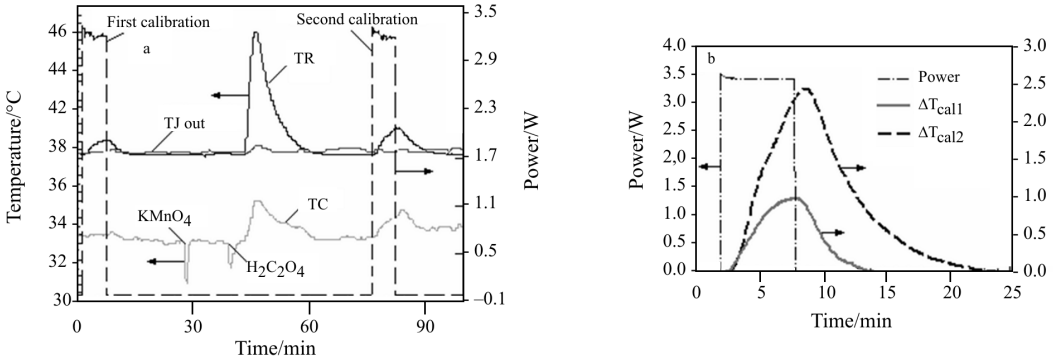

Fig. 3 Acrylamide polymerization at 39°C with $KMnO_4/H_2C_2O4$ redox system in 10% aqueous solution: a – plots of the acquired raw data (P_{stirr} and TJ_in are not shown); b – the effect of viscosity increase on the heat transfer coefficient, *UA*. For both calibrations the amount of heat dissipated by the calibration probe was the same, 1200 J

period, t_{cal}, resulting in a temperature increase. The heat generated during the calibration is equal to:

$$Q_c = P \cdot t = UA \int_0^{t_{cal}} \Delta T_R \, dt + UA \cdot S^* \qquad (4)$$

where S^* is the area of the calibration peak (°C s). After calibration the determination of reaction heat, Q_r, is very easy: $Q_r = Q_c \cdot S/S^*$; where S is the integral of reaction effect. The calibration is performed before and after reaction experiment. When the difference between the areas is significant, as in the case of polymerization reactions (Fig. 3b), the two values of the heat transfer coefficient are interpolated to obtain the desired $UA(t)$ profile, which is subsequently used for determination of the heat of reaction.

Results and discussion

Construction of solid-liquid phase diagrams in ternary systems

For the different investigated systems the experimental mole fractions x_1, x_2 and x_3, represent the component 1, the solid solute, component 2, water (H_2O), and component 3, the alcohol, methanol (MeOH), ethanol (EtOH) or propanol (PrOH), respectively. Graphical representation of the measured data are shown in Figs 4a–c. In these Figures the smoothed curves have been obtained through the procedure described in what follows. The original raw data are respectively the amount (in mass w_1) of solute 1, the volume of the aqueous mixed solvent (water + alcohol) in which the amount w_2 of water is known as well as the amount w_3 of alcohol. Densities of water-alcohol mixtures were taken from literature [15] to evaluate the respective quantities of water and alcohol in the injected volumes of solvent. From the different mass w_i the corresponding mole fractions were calculated; they constitute the experimental data to be

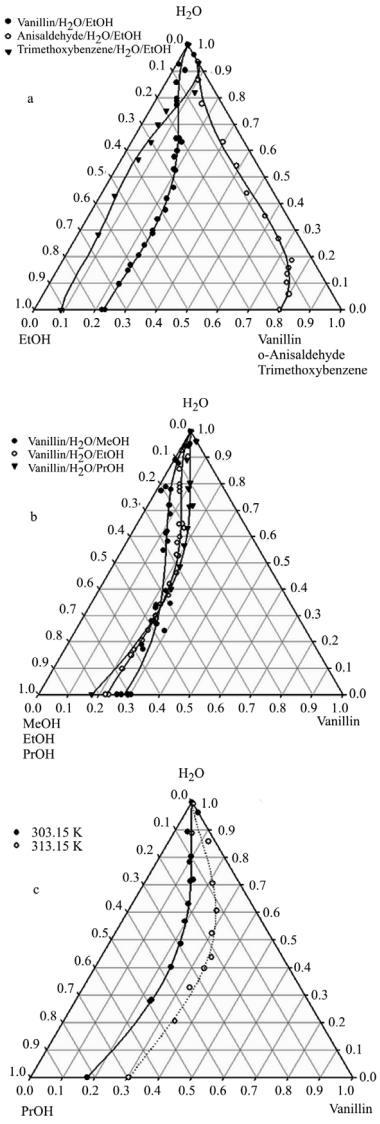

Fig. 4 Ternary plots for the investigated systems: a – effect of the solute nature on the equilibrium lines for a water/ethanol mixture; b – effect of the polarity of the solvent mixture on the dissolution of vanillin at 303.15 K; and c – effect of temperature on the dissolution of vanillin into water/propanol mixtures

treated in order to get the fitting equations to represent the solid-liquid equilibrium lines for the different systems. Firstly, a plot of x_1 *vs*. x_2 was fitted with the following polynomial y:

$$x_1 = f(x_2) = y = \sum_{i=0}^{n} a_i (1 - x_2)^i \quad (5)$$

Coefficients a_1 were adjusted to give the best fit. Secondly, using polynomial y a table of numerical values X_3 is generated as a function of X_2, $X_3 = f(X_2)$, at rounded values of X_2 (e.g. $0 \le X_2 \le 1$ at 0.05 increments) using the relation: $X_3 = 1 - x_1 - X_2$, where $x_1 = y = f(X_2)$ as given by Eq. (5) and $x_1 + X_2 + X_3 = 1$.

This 'normalization' step allows then to draw the smoothed curves in Figs 4a–c. Equation (5) is the actual fitting equation of the experimental data points. The best fit has been obtained using a SigmaPlot software which gives automatically the solubility maximum of the solid in the optimal composition of the aqueous mixture. The coefficients a_i and corresponding standard deviations σ are listed in Table 2.

Homogeneous solution polymerization of acrylamide. From measured signals to reliable calorimetric data

It is well known that the aqueous solutions of poly(acrylamide) exhibit high viscosities. The modification of viscosity during the reaction induces large changes in heat transfer coefficient. In this case, the heat of reaction cannot be computed from Eq. (1), which is one of the limitations of reaction calorimetry for polymerization reactions. As Fig. 3b shows, at the end of polymerization the increase of temperature is more than three times higher (as well the surface area of the calibration effect) than the initial increase of temperature for the same amount of heat supplied in the reaction mass. Taking into account Eq. (4) this means that the *UA* strongly decreases during the experiment. A simplified and common way of approaching the problem is by performing two calibration experiments, before and after the reaction. The two values of the heat transfer coefficient are thus interpolated, by obtaining the desired $UA(t)$ profile. As is seen in Fig. 5b and Table 3, the quality of results depends heavily on the interpolation procedure used (i.e. average value, linear with time, proportional to conversion, proportional to the power input of the stirrer).

On the other side, the reliability of kinetic data is influenced not only by the precision of the signals measurement, but also by thermogenesis [16]. Several methods have been proposed for the deconvolution of thermokinetic data and we used a differentiation method based on the convolution of the measured

Table 2 Coefficients of the fitting Eq. 5 and corresponding standard deviations σ used to represent the smoothed curves in Fig. 4. The temperature was 303.15 K

Ternary system	a_0	a_1	a_2	a_3	a_4	a_5	σ
Vanillin/H_2O/MeOH	–	0.0060	1.1346	–1.0615	0.2023	–	0.0189
Vanillin/H_2O/EtOH	–	0.1037	1.7322	–2.8849	1.2743	–	0.0087
Vanillin/H_2O/PrOH	–	0.4354	0.5372	–1.3635	0.5659	–	0.0080
Vanillin/H_2O/PrOH*	–	0.6449	0.8499	–2.3078	1.1189	–	0.0145
o-Anisaldehyde/H_2O/EtOH	0.0292	0.4758	0.4811	0.7530	–0.9381	–	0.0097
Trimethoxybenzene/H_2O/EtOH	–	1.5758	–8.8622	19.429	–18.480	6.4261	0.0139

*313.15 K

Table 3 Evolution of the overall heat transfer coefficients, *UA*, of the calorimeter time constants, τ, and of heat of polymerization, ΔH_R, in function of the interpolation method used to describe the variation of *UA* during the polymerization of AM in water*

Measured parameters		Units	Values
Overall heat transfer	Before polymerization, UA_1	*W*/ºC	3.409
coefficient, *UA*	After polymerization, UA_2	*W*/ºC	1.402
Time constant, τ	Before polymerization, τ_1	s	92
	After polymerization, τ_2	s	268
Heat of reaction, ΔH_R,	Average of UA_1 and UA_2, *Avr*		88.20
estimated as follows:	Proportional with time, *P*_Time	kJ mol^{-1} AM	102.53
	Proportional to conversion, *P*_Conv		88.21
	Proportional to power input of stirrer, *P*_Stirrer		72

* Reaction conditions are given in Fig. 3.

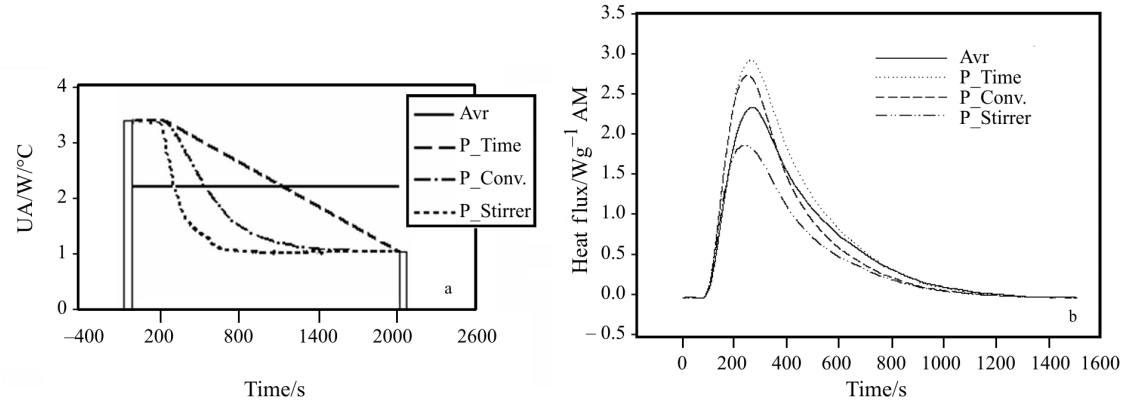

Fig. 5 Different interpolation procedures used for describing the profile of UA during the a – experiment and b – evolution of heat released during polymerization in function of interpolation method

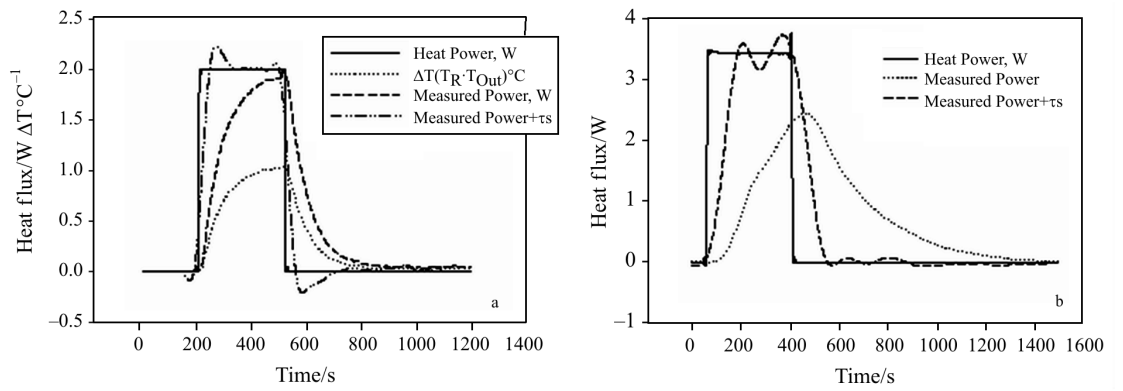

Fig. 6 Effect of deconvolution on the measured heat of calibration compared with the supplied heat pulse, a – before and b – after polymerization

heat flow $W(t)$ by the generated one $\phi(t)$ represented by the following system of linear equations:

$$\phi(t)=\phi(t)+\tau_1\frac{d\phi(t)}{dt}$$
$$\phi(t)=\phi(t)+\tau_2\frac{d\phi_1(t)}{dt} \quad (6)$$
$$\phi(t)=\phi(t)+\tau_n\frac{d\phi_{n-1}(t)}{t}.....$$

where $W(t)=\lim_{n\to\infty}\phi(t)$and τ_1, τ_2,…. τ_n are calorimeter time constants of successive orders. In practical cases, a limited number (usually one) of linear equations is used. The parameters of the equations can easily determined by heat pulse calibration concomitantly with heat transfer coefficient determination, see Table 3. The effect of the first-order deconvolution on the shape heat measured during the two calibrations is illustrated in Fig. 6.

Isothermal titration calorimetry

Between the investigated benzene substituted compounds, vanillin is a product of technological importance which is produced industrially in large amounts. The ultimate step in the production line is its crystallization in an appropriate solvent in order to obtain an end product in the form of pure small crystals. Water-alcohol binary mixtures are certainly the most suitable solvents in terms of cost and recycling feasibility. From the present study general conclusions can be drawn as illustrated in the ternary phase diagrams Figs 4a–c. The influence of the chemical structure of the solute on its solubility is shown in Fig. 4a. At a given temperature (303.15 K) and in water-ethanol binary solvent *o*-anisaldehyde is much more soluble than vanillin and 1,3,5-trimethoxybenzene, respectively. At 303.15 K Fig. 4b shows that vanillin is more easily solubilized in water/methanol mixture than in water/ethanol or water/propanol when the solutions are rich in alcohols and interestingly the situation is changed if the water prevails in the solvent mixture. The crossing point of the three solubilization curves is located at about 0.45 mole water/mole alcohol. As expected, for the same compound and solvent mixture, temperature has a distinct influence on the solubilization, Fig. 4c. The increase of temperature with 10 K

(from 303.15 to 313.15 K) induces the increase of solubility of about 30% and less alcohol is necessary.

In conclusion, isothermal titration calorimetry can be recommended as a convenient technique to obtain non only a qualitative description of solid-liquid phase diagrams in ternary systems, but also precise concentrations of the components along the solid-liquid line. The fitting equations developed to represent this line can be used for engineering calculations.

Reaction calorimetry

As mentioned in the introduction, the above-described RC was designed to determine the essential parameters of polymerization reactions. The most important parameter is the reaction rate, which is calculated from the heat generated by polymerization.

The radical polymerization of acrylamide in aqueous media was chosen as model reaction to characterize the calorimeter, since it is known as a reproductive and easy to led reaction, and well described in literature. As shown in Fig. 3a, the polymerization starts soon after the dosing of the second component of the redox system, i.e. the oxalic acid. The polymerization occurs rather fast and the maximum increase of temperature of the reaction mass ($\Delta T_R = T_R - T_J$ out) was about 7.3°C. The values of heat of polymerization, ΔH_R, (Fig. 5b and Table 3), are influenced by the interpolation method used to describe the profile of *UA*. The highest values were always found when the *UA* varies proportional with time since the reaction rate is higher just at the beginning of polymerization and the values of $UA(t)$ are closer to UA_1. Surprisingly, in all cases the values of ΔH_R, are the same for proportional to conversion and average value interpolation methods, event if the heat release faster occurs in the first case. It is worth mentioning that this value is in fairly good concordance with the one reported in literature, i.e. 89.6 kJ mol^{-1} [17], irrespective of the initial monomer concentration or temperature. The lowest values of ΔH_R, have been obtained when proportional to the power input of stirrer interpolation method was used to calculate $UA(t)$ variation. Figure 7(a) illustrates the process evolution evaluated through the heat released and the power uptake by the stirrer engine. Clearly, the increase of viscosity is faster monitored by the system as the heat released during polymerization. This behavior is related both to the relatively long time constant of the calorimeter (of about 100 sec) and to the sensitivity of measurement of power uptake of stirrer.

The results of deconvolution of measured data (Table 3) show that the time constant of calorimeter strongly increases, from 92 to 268 s, with the decrease of *UA* induced be the change of viscosity. As seen in Fig. 7b, the reconstructed curves of measured heat flux match with enough accuracy the heat flux profile for the two calibration experiments, before and after reaction. As soon as the time constants before and after polymerization are determined, the method allows to reconstruct the profile of heat flux during polymerization. In this figure the reconstructed curves supposing a variation of time constant proportional to conversion or considering the average value of the time constants are compared to the corresponding profiles obtained when only the variation of *UA* was taken into account. As expected, the profile of heat released during polymerization is strongly influenced by the variation of $\tau(t)$ even if the heat of reaction is the same. For an accurate kinetic interpretation of the

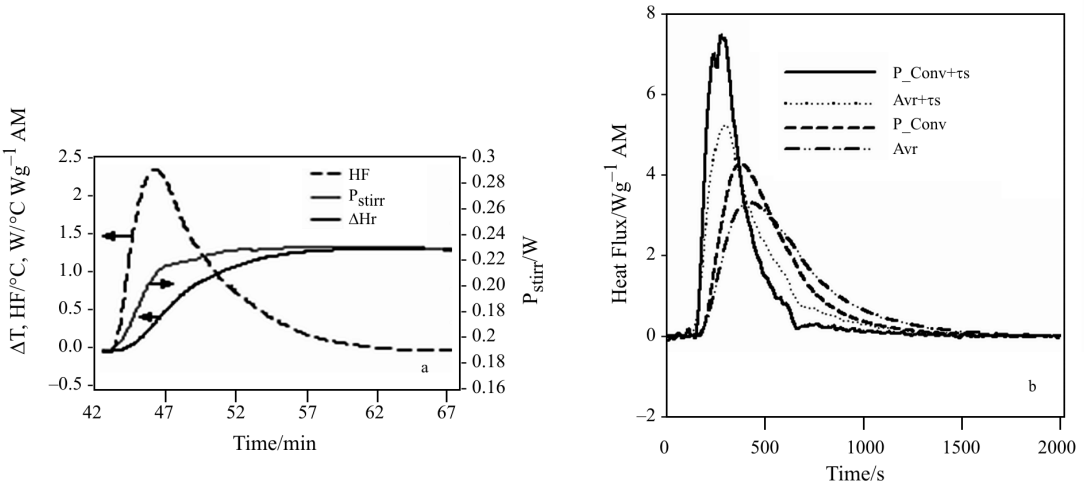

Fig. 7 Comparison between the advancement of polymerization monitored by the increase of power input of the stirrer and the integral of a – heat released and b – comparison between the reconstructed, after deconvolution of the signal, and the measured heats of polymerization. In both cases the interpolation procedures used for describing the profile of *UA* were proportional to conversion and the average value of *UA* before and after experiment

data the evolution of the time response of the apparatus during the experiment must be considered.

Temperature oscillation calorimetry

The problem of a correct calorimetric evaluation despite a changing of heat transfer value may be solved using temperature oscillation calorimetry (TOC). This technique makes only use of the reactor energy balance and determines already during the reaction the heat transfer value from forced temperature oscillations. This new method to determine the chemical heat flow simultaneously to a changing heat transfer value requires only the use of a mathematical procedure for evaluation of measured data [18].

In the present work a highly sensitive differential calorimeter (BGR-Tech, Poland) was used to perform TOC measurements. The desired oscillations of temperature were obtained by imposing a sinusoidal variation of the set-point of calorimetric block by means of an external temperature control system. The amplitude of temperature oscillations was between 0.25 and 0.5°C and the period of oscillation was 6 min.

The evaluation of energy balance Eq. (1) is performed in two steps. In the first step the heat transfer value *UA* is calculated from temperature oscillations. In the second step the reactor energy balance without oscillating heat contribution is considered and the chemical heat flow, Q_{Chem}, is calculated from Eq. (1). Given that Eq. (7) is the general expression for an oscillating signal, and considering only the influence of oscillating terms on energy balance the equations for *UA* (Eq. (8)) and heat capacity c_p (Eq. (9)) are obtained [19]:

$$X = Axe^{i(\omega t + \varphi x)} \tag{7}$$

$$UA = \frac{A_Q}{A_T}\cos(\varphi_Q - \varphi_T) \tag{8}$$

$$mc_p = \frac{A_Q}{\omega A_T}\sin(\varphi_Q - \varphi_T) \tag{9}$$

The values of phase and amplitude for each signal during the course of chemical reaction can be obtained applying the Fourier transform technique on each measured signal.

As model reaction the neutralization reaction of H_2SO_4 (0.5 N) with NaOH (0.5 N) was selected, which is known as highly exothermic reaction (–139.1 kJ mol^{-1}). The dosing period of NaOH was 80 min. The raw data of a typical run and the *UA* and Q_{Chem} evolution during the experiment are illustrated in Figs 8a–d.

As expected, the overall heat transfer coefficient, *UA*, increases almost linearly during the experiment, Fig. 8c, since the wetted surface area in the reactor, *A*, increases during the dosing period. The integration of heat released during the neutralization gives an enthalpy of –133.5 kJ mol^{-1} which is close to the literature values.

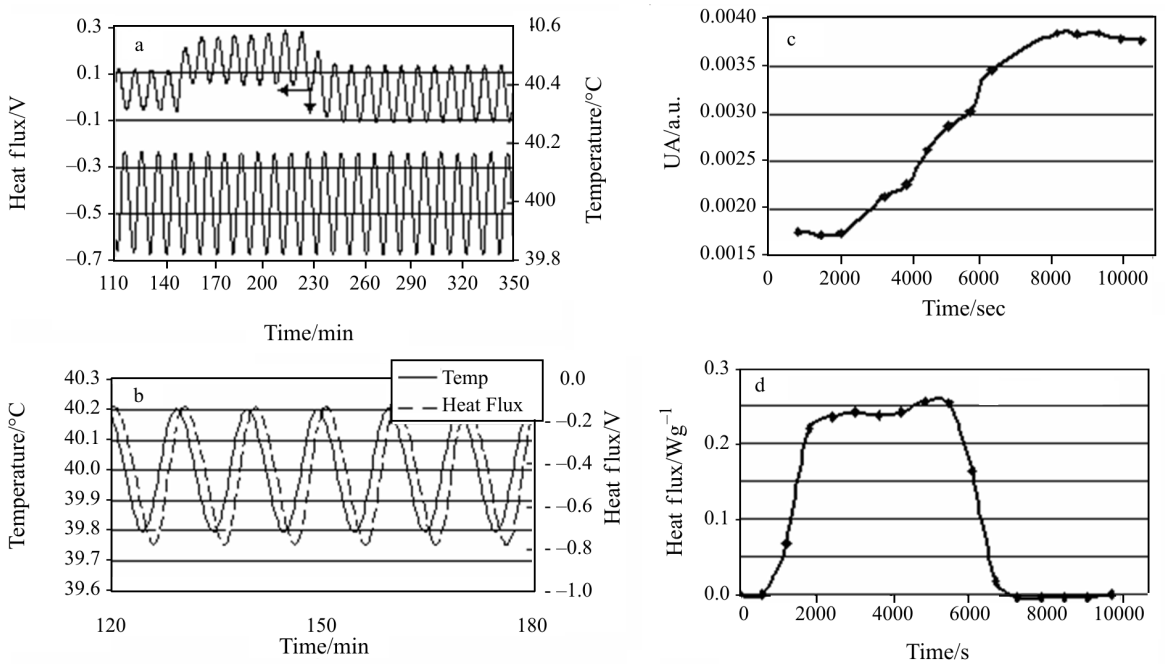

Fig. 8 Temperature oscillation calorimetry during the neutralization of 2 ml of H_2SO_4 (0.5 N) with 2 mL of NaOH (0.5 N) at 40°C: a – raw measured heat flux (upper part) and temperature (lower part); b – phase shift between the measured heat flux and temperature, respectively; c – evolution of the overall heat transfer coefficient, *UA*; and d – of the heat of neutralization in time

In conclusion, RC is a powerful technique to investigate the polymerizations processes in the near-to-the-industrial condition if a special attention is paid to the baseline determination (*UA*) and to the deconvolution of measured heat flux, and, of course, when the concomitant determination of Q_{Chem} and *UA* is possible.

References

1 S. L. Randzio, Chem. Soc. Rev. Annu. Rep. Prog. Chem. C., 27 (1998) 433.
2 N. Markova and D. Hallen, Anal. Biochem., 331 (2004) 77.
3 I. Wadsö, Chem. Soc. Rev., 26 (1997) 383.
4 D. Zeiss and A. Bauer-Brandl, J. Therm. Anal. Cal., 83 (2006) 309.
5 P. Garidel and A. Hildebrand, J. Therm. Anal. Cal., 82 (2006) 483.
6 M. M. Pierce, C. S. Raman and B. T. Nall, Methods, 19 (1999) 213.
7 T. Wiseman, S. Williston, J. F. Brandts and L. N. Lin, Anal. Biochem., 179 (1989) 131.
8 E. Freire, O. L. Mayorga and M. Straume, Anal. Chem., 62 (1990) 950.
9 D. S. Gill, D. J. Roush, K. A. Shick and R. C. Willson, J. Chromatogr. A., 715 (1995) 81.
10 D. H. Smith and G. C. Allred, J. Colloid Interface Sci., 124 (1988) 199
11 D. H. Smith and G. L. Covatch, 162 (1994) 372
12 D. H. Smith and G. L. Covatch, 171 (1995) 112.
13 P. G. De Luca and C. Scali, Chem. Eng. Sci., 57 (2002) 2077.
14 M. Lathi, A. Avela and J. Seppälä, Thermochim. Acta, 262 (1995) 33.
15 G. C. Benson and O. Kiyohara, J. Solution Chem., 9 (1980) 791.
16 L. Vincent, N. Sbirrazuoli and S. Vyazokin, Ind. Eng. Chem. Res., 41 (2002) 6650.
17 J. Brandurp and E. H. Immergut Eds., 'Polymer Handbook', John Wiley and Sons, Inc., New York, 1975, p. 273.
18 A. Tietze, I. Ludke and K.-H. Reichert, Chem. Eng. Sci., 51 (1996) 3131.
19 J. Sempere, R. Nomen, E. Serras and J. Sales, J. Therm. Anal. Cal., 52 (2003) 65.

DOI: 10.1007/s10973-006-7639-6